

Nonequilibrium thermal boundary layer in a capillary discharge with an ablative wall

Michael Keidar^{a)}

Department of Aerospace Engineering, University of Michigan, Ann Arbor, Michigan 48109

Isak I. Beilis

Department of Interdisciplinary Study, Tel Aviv University, Tel Aviv 69978, Israel

(Received 22 September 2006; accepted 16 October 2006; published online 15 November 2006)

A thermal nonequilibrium region near wall in a capillary discharge is considered. The proposed model suggests that nonequilibrium thermal boundary layer thickness strongly depends on the capillary wall ablation rate. It is shown that the applicability of the thermal equilibrium condition, widely employed in capillary models, is limited to a case with a large ablation rate.

© 2006 American Institute of Physics. [DOI: [10.1063/1.2388953](https://doi.org/10.1063/1.2388953)]

Nowadays, capillary discharge plasma sources have numerous applications, including plasma thrusters,¹ energetic propellant ignition and combustion,² circuit breakers,³ soft-x-ray and extreme ultraviolet sources,^{4,5} etc. In addition, capillary discharge is a very promising source for producing preformed plasma channels that can guide high-power laser pulses.⁶ Optical guiding of high-intensity laser pulses is used in a number of applications, such as laser wake-field accelerators, x-ray lasers, harmonic generators, etc.^{7–10} Laser propagation through the plasma with constant beam size, the so-called matched beam, can occur if the diffraction term is balanced by the refraction term.¹¹ In case of the capillary sustained plasma, the matching laser beam radius is determined by the plasma density radial distribution inside the capillary.¹¹ The refraction index depends on the plasma density, and therefore the plasma column with a density profile introduces the refraction index change. Simple analysis shows that a plasma column with density minimum on axis produces a desired refractive index profile for guiding.¹¹

Two distinct types of capillary discharge were used for optical guiding, namely ablation-controlled capillary¹² and gas-filled capillary.⁷ Ablation-controlled capillary operates by ablation and ionization of the wall material, while gas-filled capillary discharge is supported by ionization of the prefilled gas, thus ionization is decoupled from the plasma-wall interactions. In both types of the capillary discharge simulations and measurements indicate that the radial plasma density profile is parabolic near the capillary exit plane.^{8,13} Since the radial plasma density profile in the capillary has primary importance for optical guiding, it was a subject of numerous studies.^{6–13} Models of the gas-filled capillary discharge were based on the premise that the radial plasma temperature distribution (and therefore the plasma density distribution) inside the capillary is determined by the energy balance between the Ohmic heating and cooling due to electron heat conductivity.^{13,14} In previous models,^{13,14} it was assumed that all plasma species are in thermal equilibrium in the entire capillary cross section, so that near the capillary wall all temperatures are equal, i.e., $T = T_i = T_e = T_a$, where T_i

is the ion temperature, T_e is the electron temperature, and T_a is the neutral particle temperature. This assumption allows obtaining a straightforward solution for the radial temperature and density profiles. While the approach proposed in Refs. 13 and 14 is reasonable in the case of the gas-filled capillary, it may not be accurate in the case of the ablation-controlled capillary discharge in which the plasma is generated as a result of wall ablation. In fact, it is known that there is a sharp gradient of plasma properties near the wall.¹⁵ The strong gradient near the wall exists because the cold vapor inflows to the plasma due to wall ablation. For instance, in the case of polyethylene capillary discharge with a pulse power of about a few MW, the plasma temperature is about 1–2 eV, while the neutral vapor temperature at the wall is about 700 K (Ref. 16). Therefore, the plasma in the near-wall region may depart from the thermal equilibrium. Since the difference between the electron temperature and the neutral vapor temperature near the wall is large, one cannot use *a priori* the thermal equilibrium assumption in the entire channel cross section. It is apparent that the temperature gradient may affect the heavy particle density distribution in the near-wall region. In this article, we analyze a general approach considering temperature nonequilibrium near the capillary wall and reexamine the assumption previously employed, i.e., thermal equilibrium in the entire channel cross section. The applicability of an assumption about the thermal equilibrium is important for modeling of the capillary discharge plasma for variety of applications.

It should be pointed out that the principal effect causing thermal nonequilibrium and sharp temperature gradient is the ablation of the wall. Ablation is determined by the velocity at the edge of the Knudsen layer, which depends on the plasma properties in the capillary bulk region.^{17,18} In the present analysis, we will study an influence of the velocity at the edge of the Knudsen layer as a parameter.

Our model considers the axisymmetric steady-state problem of the capillary discharge shown schematically in Fig. 1. Since, typically, the capillary length L is much larger than the capillary radius R , i.e., $L/R \gg 1$, one can assume that plasma parameters are uniform in an axial direction, except a region near the exit plane where significant acceleration takes

^{a)}Electronic mail: keidar@umich.edu

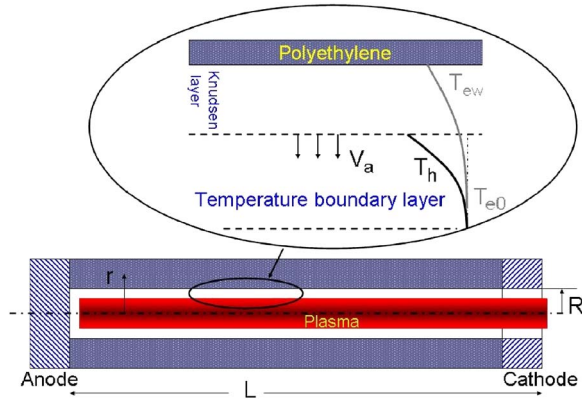


FIG. 1. (Color online) Schematic of the capillary discharge and plasma-wall transition region.

place.¹⁶ Thus, we focus on the radial distribution of the plasma parameters. We start with the energy conservation equations for neutrals and electrons in the following simple form:

$$\frac{3}{2}n_a V_a \frac{dT_a}{dr} = \frac{3m_e n_e}{m_a \tau_{eh}} (T_e - T_a), \quad (1)$$

$$\frac{3}{2}\Gamma_e \frac{dT_e}{dr} = \frac{j^2}{\sigma} - \frac{3m_e n_e}{m_a \tau_{eh}} (T_e - T_a), \quad (2)$$

where V_a is the vapor velocity at the edge of the Knudsen layer (see Fig. 1), j is the current density along the capillary, T_e, T_a are electron and atom temperatures, respectively, Γ_e is the electron flux to the wall (it is assumed that wall has a floating potential, and electron flux is determined by electron density and temperature at the sheath edge), and τ_{eh} is the electron–heavy particles collision time. Electron collision with heavy particles is the mechanism leading to thermalization between hot electrons and cold neutrals vaporized from the wall. We assume that heavy particles are in equilibrium, so that $T_i = T_a = T_h$. Ion and electron motion is determined by the electric field near the capillary walls. In the quasineutral part of the near-wall region (presheath), the plasma density can be described as follows:¹⁹

$$\frac{d}{dr}(n_e V) = \nu_{iz} n_e, \quad (3)$$

$$m_a \frac{d}{dr}(n_e V^2) = en_e E, \quad (4)$$

where ν_{iz} is the ionization frequency and V is the ion velocity (radial component).

We calculate the degree of ionization in the plasma bulk region assuming Saha equilibrium. Since there is no significant flow in the radial direction (typically $V_a/C_s \ll 1$), the pressure can be assumed to be constant in the capillary, $P(r) = n_a T_a + n_e T_e + n_i T_i = \text{const}$. It should be noted that this assumption does not preclude the existing temperature and density gradients, which cancel each other.

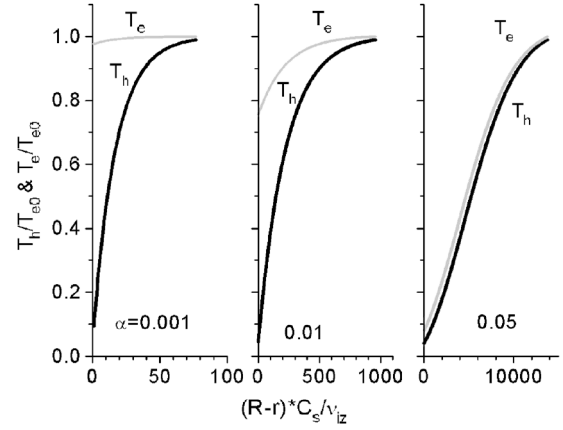


FIG. 2. Temperature distribution with velocity at the Knudsen layer edge $\alpha = V_a / \sqrt{2T_a/m_a}$ as a parameter. V_a is the atom velocity at the Knudsen layer edge (shown in Fig. 1).

Surface temperature of the capillary wall determines the vapor pressure. For instance, in the case of polyethylene the vapor pressure can be approximated as follows:^{20,21}

$$P_v = 10^5 \exp\left(A \cdot \left[\frac{1}{B} - \frac{1}{T_s}\right]\right), \quad (5)$$

where pressure P_v is in Pa, $A = 5565.22$, $B = 453$, and T_s is the surface temperature (in degrees K).

We will present a solution for the particular case of a capillary made of polyethylene and having the following geometry:³ capillary length is $L = 35$ mm and capillary radius is $R = 3$ mm. Plasma parameter distribution is calculated using the capillary model described elsewhere (Refs. 1, 16, and 21) for the following conditions: discharge duration is $300 \mu\text{s}$ and sinusoidal current waveform with a current peak of about 2.6 kA. In this case, the following values are predicted for polyethylene surface temperature and plasma parameters: surface temperature is about $T_s = 700$ K, electron temperature is about $T_e = 1.5$ eV, and plasma density peak is

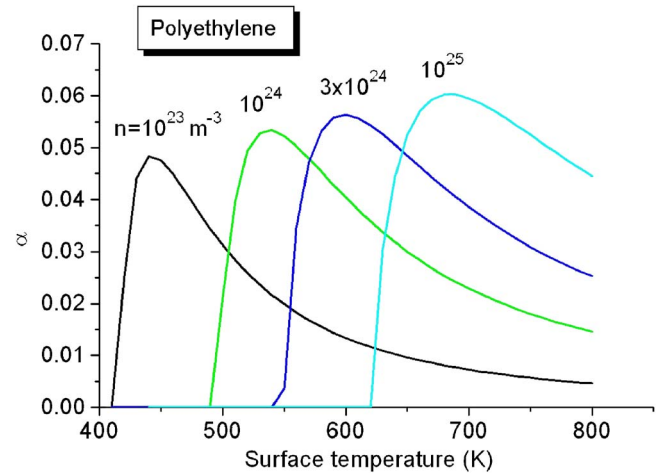


FIG. 3. Parameter α as a function of polyethylene surface temperature with density in the plasma bulk as a parameter.

about 10^{25} m^{-3} . Note that the velocity at the Knudsen layer edge V_a (parameter α) depends on the axial position along the capillary and thus in the present radial model can be considered as a free parameter.²¹

Electron and heavy particle temperature distributions are shown in Fig. 2 with normalized velocity V_a as a parameter. One can see that parameter α (which is the normalized velocity at the edge of the Knudsen layer) significantly affects the temperature distribution. According to the calculation shown in Fig. 2, the thickness of the plasma nonequilibrium region (i.e., the region with $T_h < T_e$) is much larger than the effective mean free path determined as C_s / ν_{iz} . Larger parameter α leads to a thinner temperature nonequilibrium region. It is important to note that in the case of a large parameter α , the electron and the heavy particle temperatures are in equilibrium, while electron temperature at the wall is reduced due to intensive cooling.

Recall that in general, the parameter α is determined by the capillary discharge parameters such as plasma density, electron temperature, capillary wall surface temperature, capillary wall material, as well as position along the capillary (Refs. 1, 16, and 21). This parameter can be calculated in the framework of the ablation model described elsewhere.^{22,23} Typical dependence of the parameter α on the surface temperature is shown in Fig. 3 with plasma density as a parameter. One can see that the maximum parameter α is small, i.e., velocity at the edge of the Knudsen layer is much smaller than the sound speed. Maximum velocity slightly increases with the plasma density increase. Based on typical values of the parameter α shown in Fig. 3 and calculations of the temperature boundary layer shown in Fig. 2, one can conclude that the thermal equilibrium approximation cannot always be justified.

In summary, analysis of the thermal nonequilibrium region in the capillary discharge suggests that the nonequilibrium region thickness depends strongly on the ablation regime. The temperature equilibrium condition in the entire capillary channel can be used if the velocity at the Knudsen layer edge is relatively large, i.e., $\alpha \geq 0.05$. In other words,

the applicability of the thermal equilibrium assumption, widely accepted in the capillary discharge modeling, is limited to cases with higher ablation rates.

This work was sponsored in part by the Army Research Office.

- ¹M. Keidar, I. D. Boyd, and I. I. Beilis, *IEEE Trans. Plasma Sci.* **28**, 376 (2000).
- ²R. A. Beyer and R. A. Pesce-Rodriguez, *IEEE Trans. Magn.* **39**, 207 (2003).
- ³E. Domejean, P. Chevrier, C. Fievet, and P. Petit, *J. Phys. D* **30**, 2132 (1997).
- ⁴S. V. Kikhlevsky, J. Kaiser, O. Samek, M. Liska, and J. Erostryak, *J. Phys. D* **33**, 1090 (2000).
- ⁵D. Hong, R. Dussart, C. Cachoncinlle, W. Rosenfeld, S. Gotze, J. Pons, R. Viladrosa, G. Fleurier, and J. M. Pouvesle, *Rev. Sci. Instrum.* **71**, 15 (2000).
- ⁶D. Kaganovich, P. Sasorov, C. Cohen, and A. Zigler, *Appl. Phys. Lett.* **75**, 772 (1999).
- ⁷D. J. Spence and S. M. Hooker, *Phys. Rev. E* **63**, 015401(R) (2000).
- ⁸M. Levin, G. Marcus, A. Pukhov, A. Zigler, and P. Sasorov, *J. Appl. Phys.* **93**, 851 (2003).
- ⁹H. M. Milchberg, C. G. Durfee III, and T. J. McIlrath, *Phys. Rev. Lett.* **75**, 2494 (1995).
- ¹⁰D. V. Korobkin, C. H. Nam, and S. Suckewer, *Phys. Rev. Lett.* **77**, 5206 (1996).
- ¹¹R. F. Hubbard, D. Kaganovich, B. Hafizi, C. I. Moore, P. Sprangle, A. Ting, and A. Zigler, *Phys. Rev. E* **63**, 036502 (2001).
- ¹²Y. Ehrlich, C. Cohen, A. Zigler, J. Krall, P. Sprangle, and E. Esarey, *Phys. Rev. Lett.* **77**, 4186 (1996).
- ¹³N. A. Bobrova, A. A. Esaulov, J. I. Sakai, P. V. Sasorov, D. J. Spence, A. Butler, S. M. Hooker, and S. V. Bulanov, *Phys. Rev. E* **65**, 016407 (2001).
- ¹⁴V. V. Ivanov, K. N. Koshelev, E. S. Toma, and F. Bijkerk, *J. Phys. D* **36**, 832 (2003).
- ¹⁵J. Ashkenazy, R. Kipper, and M. Caner, *Phys. Rev. A* **43** 5568 (1991).
- ¹⁶M. Keidar, I. D. Boyd, and I. I. Beilis, *J. Propul. Power* **19**, 424 (2003).
- ¹⁷C. J. Knight, *AIAA J.* **17**, 519 (1979).
- ¹⁸I. I. Beilis, *IEEE Trans. Plasma Sci.* **34**, 855 (2006).
- ¹⁹M. Keidar and I. I. Beilis, *IEEE Trans. Plasma Sci.* **33**, 1481 (2005).
- ²⁰H. Orbey, C. P. Bokis, and C. C. Chen, *Ind. Eng. Chem. Res.* **37**, 4481 (1998).
- ²¹M. Keidar and I. D. Boyd, *J. Appl. Phys.* **99**, 053301 (2006).
- ²²M. Keidar, I. D. Boyd, and I. I. Beilis, *J. Phys. D* **34**, 1675 (2001).
- ²³M. Keidar, J. Fan, I. D. Boyd, and I. I. Beilis, *J. Appl. Phys.* **89** 3095 (2001).